ACS APPLIED MATERIALS & INTERFACES

Research Article

www.acsami.org

Self-Stratified Antimicrobial Acrylic Coatings via One-Step UV Curing

Jie Zhao,[†] William Millians,[‡] Saide Tang,[§] Tiehang Wu,[‡] Lei Zhu,[§] and Weihua Ming*[,†]

[†]Department of Chemistry, Georgia Southern University, P.O. Box 8064, Statesboro, Georgia 30460, United States

[‡]Department of Biology, Georgia Southern University, P.O. Box 8042, Statesboro, Georgia 30460, United States

[§]Department of Macromolecular Science and Engineering, Case Western Reserve University, Cleveland, Ohio 44106, United States

ABSTRACT: We designed and synthesized a novel quaternary ammonium methacrylate compound (QAC-2) bearing a perfluoroalkyl tail on one end and an acrylic moiety on the other. Via one-step UV curing of QAC-2 and methyl methacrylate (MMA) with ethylene glycol dimethacrylate (EGDMA) as the cross-linker, we obtained cross-linked coatings with excellent antimicrobial property, as demonstrated by the total kill against both Gram-negative *Escherichia coli* (*E. coli*) and Gram-positive *Staphylococcus epidermidis* (*S. epidermidis*) at a QAC-2 concentration as low as ~0.06 mol % (~0.4 wt %) relative to MMA, which was substantially lower than the QAC amount needed in the coatings containing QACs with a hydrocarbon tail. A zone of inhibition test confirmed that the antimicrobial effect was on the basis of contact killing and there was no leaching of antimicrobial species from the cross-linked coating. The high antimicrobial potency in QAC-2-containing films was the consequence of strong surface enrichment of the fluorinated QAC, as confirmed by X-ray photoelectron spectroscopy (XPS).

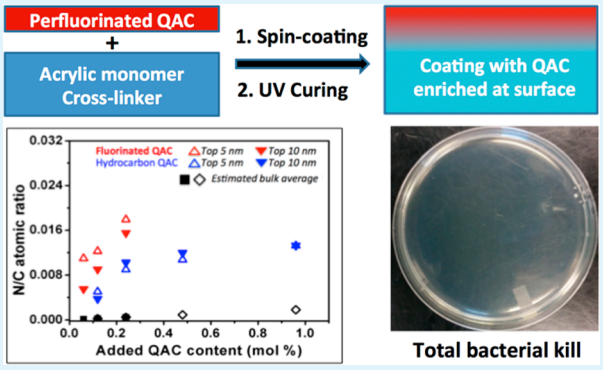

KEYWORDS: *Antimicrobial coating, self-stratification, quaternary ammonium compound (QAC), perfluorinated reactive QAC, UV curing*

INTRODUCTION

Effective antimicrobial coatings are highly desired in medical- or health-related areas to prevent growth and proliferation of pathogenic bacteria on substrate surfaces. Various approaches have been explored to obtain coatings with competent antimicrobial properties.[1−12] A commonly used approach is to incorporate antimicrobial agents such as silver ions,[9−12] antibiotics,[13,14] quaternary ammonium compounds (QACs),[15,16] and halogens[17−19] into a coating, and the antimicrobial activity mainly relies on the slow release of the bactericidal agents into the surroundings. However, the antimicrobial property will diminish over time due to the exhaustion of these active biocides. Moreover, leaching of toxic biocides and heavy metals into the surroundings would cause environmental concerns as well as trigger antibiotic resistance.[20,21] Therefore, there has been increasing interest in designing antimicrobial coatings on the basis of contact kill (i.e., without releasing bactericidal substances), and various antimicrobial polymeric materials with chemically bonded antimicrobial moieties have been successfully prepared.[22] QACs, especially those with long hydrophobic tails, have been extensively investigated due to their effective antimicrobial property by exerting a strong electrostatic interaction with negatively charged bacterial cell membrane.[23−34]

Antimicrobial activity is essentially a surface property; therefore, there is no need for antimicrobial moieties to be present throughout the bulk of a coating, which may not only alter bulk property (such as moisture sensitivity) of the coating but also lead to inefficient use of antimicrobial moieties. Thus, it is highly desirable to develop coatings with optimal antimicriobial performance while using minimal amounts of antimicrobial agents (thus, unaltered bulk coating properties). We previsouly developed antimicrobial polyurethane coatings by covalently bonding QAC-containing, low surface energy reactive compounds to a polyurethane network;[35] the low surface energy enabled the QAC moiety to strongly enrich at the coating surface, leading to excellent antimicrobial coatings at low QAC loadings.

Here we report the design and synthesis of a new reactive QAC, with a perfluoroalkyl tail on one end and a methacrylate moiety on the other, which was then covalently incorporated into a cross-linked acrylic coating via one-step UV curing (Scheme 1). The surface enrichment of the fluorinated QAC was examined by contact angle analysis and X-ray photoelectron spectroscopy (XPS), and the antimicrobial performance was evaluated.

EXPERIMENTAL SECTION

Materials. Monomers including 2-(dimethylamino) ethyl methacrylate (DMAEMA, 98%) and ethylene glycol dimethacrylate (EGDMA, 99%) and a UV initiator 2-hydroxy-4-(2-hydroxyethoxy)-

Received: May 27, 2015
Accepted: July 30, 2015
Published: July 30, 2015

 © 2015 American Chemical Society

DOI: 10.1021/acsami.5b04633
ACS Appl. Mater. Interfaces 2015, 7, 18467−18472

Scheme 1. Schematic Illustration of the Self-Stratification Process for Antimicrobial Acrylic Coatings via One-Step UV Curing Involving Reactive Hydrocarbon QAC-1 (a) or Perfluorinated QAC-2 (b)

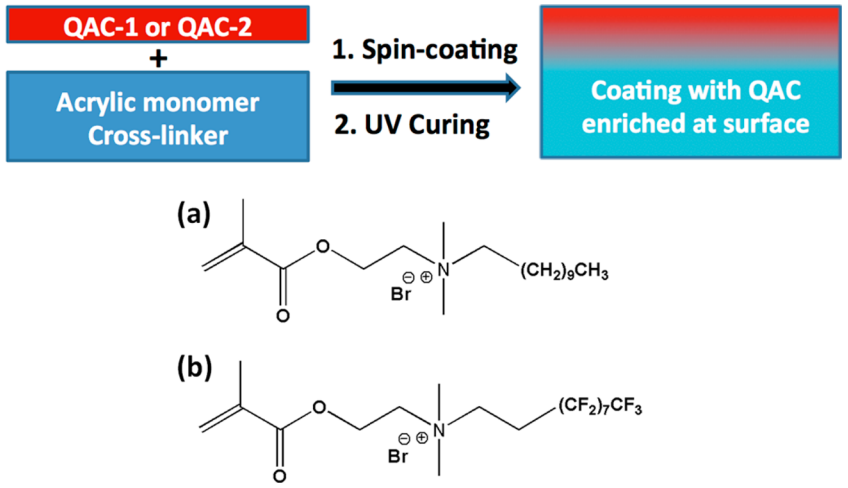

2-methylpropiophenone (HHMP, 98%) were purchased from Aldrich, methyl methacrylate (MMA, 99%) and 1-bromoundecane (98%) were from Alfa Aesar, and 1*H*,1*H*,2*H*,2*H*-perfluorodecyl bromide (PFDB, 99%) was from Oakwood Chemical Products, Inc. Solvents including acetonitrile and chloroform were obtained from Fisher and used as received. Inhibitor was removed from MMA and EGDMA by passing through an aluminum oxide column.

Synthesis of QAC-1 and QAC-2 Monomers. Two QAC-containing monomers, QAC-1 and QAC-2 (Scheme 1), were synthesized by one-step quaternization reaction. QAC-1 was prepared by reacting 0.35 g of DMAEMA (2.2 mmol) with 0.48 g of 1-bromoundecane (2.0 mmol). The starting compounds were dissolved in 10 mL of acetonitrile to obtain a uniform solution, which was then purged with argon for 20 min to remove the dissolved oxygen and magnetically stirred for 12 h at 50 °C. Then the solvent was removed by using a rotary evaporator, and the residue was dried in a vacuum oven for 24 h at 40 °C to obtain a wax-like product, QAC-1. Yield: 0.65 g (83.0%). δ_H (400 MH_Z, $CDCl_3$): 0.91 (3H, m, CH_3−CH_2−), 1.27−1.37 (18H, m, −$(CH_2)_9$−), 1.98 (3H, s, CH_3−C(C═O)═C−), 3.51 (s, 6H, $(CH_3)_2$−N^+−), 3.61 (2H, m, −C−CH_2−N^+−), 4.20 (2H, m, −O−CH_2−CH_2−N^+−), 4.71 (2H, m, −O−CH_2−CH_2−N^+−), 5.72 and 6.21 (2H, s, CH_2═C−COO−). LS-MS: *m*/*z*, $[M - Br]^+$ = 312.

Following the same procedure, QAC-2 was prepared using PFDB (1.06 g, 2 mmol) instead of 1-bromoundecane with a yield of 67.1%. δ_H (400 MH_Z, $CDCl_3$): 1.99 (3H, s, CH_3−C(C═O)═C−), 2.91 (6H, s, $(CH_3)_2$−N^+−), 3.46 (2H, m, −O−CH_2−CH_2−N^+−), 4.75 (2H, m, −O−CH_2−CH_2−N^+−), 5.72 and 6.21 (2H, s, CH_2═C−COO−). LS-MS: *m*/*z*, $[M - Br]^+$ = 604.

Preparation of QAC-1 and QAC-2 Containing Cross-Linked Coatings. Glass slides (2.2 cm × 2.2 cm) were cleaned by sonication in acetone for 10 min, followed by heating in the piranha solution (98% sulfuric acid and 35% hydrogen peroxide, 3:7 v/v) for 60 min at 90 °C. Then the glass slides were washed thoroughly with water and dried by argon flow. QAC-containing acrylic coatings were obtained from a series of mixtures containing 1.01 g of MMA (10 mmol), different QAC concentrations (ranging from 0.12 to 0.96 mol % for QAC-1 and from 0.06 to 0.24 mol % for QAC-2 with respect to MMA), 0.02 g of EGDMA (0.1 mmol), and 0.045 g of HHMP (0.2 mmol) with 1.5 mL of chloroform as the solvent. The mixture was first spin coated on a clean glass slide at 1000 rpm for 15 s and then cured by UV irradiation (F300S, 365 nm, 400 W, Heraeus Noblelight America, LLC) for 40 s to obtain the cross-linked coating. Afterward, the coating was rinsed by ethanol and deionized water and dried in a vacuum oven at 70 °C for 24 h to remove any possible unreacted monomers and trace solvent. The resulting coatings containing QAC-1and QAC-2 were labeled as Q-1 and Q-2 series, respectively, and the QAC contents in all cross-linked coatings are listed in Table 1. A coating prepared from MMA and EGDMA (free of QAC) was used as the control. The coating thickness was estimated to be 700−800 nm, as determined by atomic force microscopy (AFM) on an NT-MDT NTEGRA Prima instrument in the semicontact mode with a gold-coated cantilever NSG 10.

Table 1. Bacterial log Reduction After 24 h of Incubation with Initial Bacterial Concentration of 10^5 Bacteria/mL Treated with Q-1 and Q-2 Coatings (2.2 × 2.2 cm^2)

samples	QAC content, relative to MMA (mol %/wt %)	bacterial log reduction	
		E. coli	*S. epidermidis*
control sample[a]	0/0	0.5	0.7
Q-1-A	0.12/0.5	2	2.4
Q-1-B	0.24/0.9	2.5	3.5
Q-1-C	0.48/1.9	3	4
Q-1-D	0.96/3.8	5	5
Q-2-A	0.06/0.4	5	5
Q-2-B	0.12/0.8	5	5
Q-2-C	0.24/1.6	5	5

[a]The control sample was a cross-linked PMMA coating without QAC.

Measurements. ^{1}H NMR spectra were recorded using an Agilent 400 MHz instrument with $CDCl_3$ as the solvent. ^{1}H chemical shifts were internally referenced to the TMS signal for all spectra recorded. Positive-mode electrospray ionization mass spectrometry (ESI-MS) was carried out on a Shimadzu LCMS-2020 Single Quad instrument. All experiments were performed at ambient temperature.

X-ray photoelectron spectroscopy (XPS) measurements were performed on a PHI VersaProbe 5000 XPS Microprobe instrument using a monochromated X-ray beam and an aluminum anode (Al Kα = 1468.3 eV) at electron takeoff angles of 90° and 30° (between the film surface and the axis of the analyzer lens). The original data of carbon 1s (C_{1s}) were subjected to deconvolution analysis using XPSPEAK software. All C_{1s} peaks corresponding to hydrocarbons were calibrated at the binding energy of 285 eV to correct for the energy shift caused by charging. The fluorine to carbon (F/C) and the nitrogen to carbon (N/C) atomic ratios were determined from curve-fitted C_{1S} window spectra, according to different carbon environments.

Surface wettability of the coatings was examined on a Ramé-Hart 290 instrument. Advancing and receding contact angles (CA) for water (surface tension γ = 72.2 mN/m) and static CAs for hexadecane (γ = 27.4 mN/m) were collected at room temperature (about 20 °C).

DOI: 10.1021/acsami.5b04633
ACS Appl. Mater. Interfaces 2015, 7, 18467−18472

The CAs were averaged values measured at 3−4 different points on each sample surface.

Antimicrobial Procedure. Antimicrobial tests were performed according to a standard antimicrobial susceptibility test protocol such as ISO 22196 and JIS Z 2801. Briefly, cultures of *Escherichia coli* (*E. coli*, Carolina #155065A) and *Staphylococcus epidermidis* (*S. epidermidis*, Carolina #155556) were grown aerobically at 37 °C (24 h) in sterile Luria−Bertani (LB) broth. The bacterial concentration in the broth was determined by a cell counter. These active growing cultures were diluted in sterile distilled water to obtain a concentration of 10^5 bacteria/mL, 10 mL aliquots of bacteria suspensions were transferred to sterile plates containing Q-1 and Q-2 coatings, and a PMMA coating without QAC was used as the control. After 24 h incubation at 37 °C, the suspensions were appropriately diluted and each dilution (500 μL) was plated onto each sterile LB agar (LB broth and agar 20 g/L) culture plates, which were incubated at 37 °C overnight to give visible colonies. The number of colonies on each plate was calculated to obtain the corresponding concentration of living bacteria. Each experiment was performed in triplicate, and the reported results were averaged values.

Possible leaching of antimicrobial species from the coatings was examined by the zone of inhibition test. Cultures of *E. coli* and *S. epidermidis* were grown on sterile LB agar. The Q-1 and Q-2 coatings were placed upon the lawns with the active coating side in contact with the LB agar. After 24 h incubation at 37 °C, the possible zone of inhibition was evaluated. Any leaching of the antimicrobial species would result in an inhibition zone without bacteria growth around the coating.

RESULTS AND DISCUSSION

Surface Wettability of Q-1 and Q-2 Coatings. We prepared a series of cross-linked acrylic coatings (Q-1 and Q-2) with different QAC contents (QAC-1 and QAC-2) via fast, one-step UV curing, with the antimicrobial moiety covalently bonded to the cross-linked network. Due to the much lower surface energy of the perfluoroalkyl tail (QAC-2) than its hydrocarbon counterpart (QAC-1), the perfluorinated antimicrobial moiety may become more enriched at the coating surface. We collected contact angles for water and hexadecane on these coatings to examine their surface wettability.

As shown in Figure 1, the advancing (θ_a) and receding (θ_r) water CAs on the control sample, a cross-linked PMMA coating, were 94° and 55°, respectively. For the Q-1 series, increasing the QAC-1 content in the coating led to a gradual decrease in water CAs (Figure 1a), reaching low values of 60°/25° (θ_a/θ_r) for the coating with about 0.96 mol % QAC-1. While a long hydrocarbon tail would normally increase the water CA, the more hydrophilic quaternary ammonium moiety would lead to the opposite. The fact that much lower CAs were observed on the Q-1 coatings indicates that QAC-1 was enriched at the coating surface, which was further confirmed by the XPS analysis below. The driving force for the surface segregation of QAC-1 obviously came from the hydrocarbon tail, though it may not be as strong as in the Q-2 coatings.

A similar trend was observed for the water CAs on the Q-2 coatings (Figure 1b). Interestingly, the reduction of the θ_r was much more significant, already reaching 12° at the added QAC-2 concentration of 0.12 mol %, despite the fact that a very hydrophobic perfluoroalkyl group is connected to the quaternary ammonium moiety. This is quite different from what we reported on a polyurethane (PU) coating containing a perfluorinated QAC,[35] where an increase of θ_a was accompanied by the decrease of θ_r as the QAC content increased. This is likely due to a combination of the following factors: (1) the surface F/C atomic ratio in the UV-cured coatings (shown below) was much greater than the thermally cured PU coating, leading to more hydrophilic quaternary ammonium moiety at the coating surface, and (2) UV curing is much more rapid than thermal curing, resulting in very rapid immobilization of polymer backbones as well as dangling chains and, thus, likely random orientation of the perfluoroalkyl tails at the coating surface that might not shield the hydrophilic quaternary ammonium moiety away from water during the contact angle measurement.

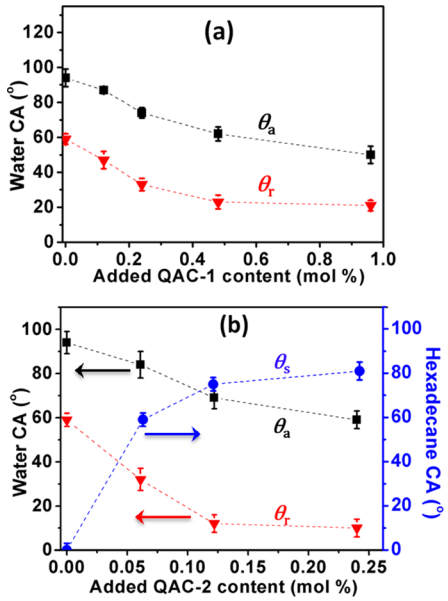

Figure 1. (a) Water contact angles on Q-1 coatings, and (b) water and hexadecane contact angles on Q-2 coatings. Dashed lines were added to guide the eye.

When the interrogating liquid was changed to hexadecane, a much different trend was observed: the static CA (θ_s) increased dramatically with the increasing content of the perfluorinated QAC, ultimately reaching 80° (on par with the values on a self-assembled perfluoroalkyl monolayer[36] and a perfluorinated PMMA[37]) at a very low QAC-2 loading (~0.24 mol %). This was a strong indication that QAC-2 was significantly segregated at the Q-2 coating surface; otherwise, the increase of hexadecane CA would be much lower (hexadecane would spread on the Q-1 coatings irrespective of the QAC-1 contents). Incorporation of a higher amount of QAC-2 would be unnecessary due to the strong surface enrichment of QAC-2 at the coating surface in the Q-2 series and their excellent bacteria-killing property (shown below).

XPS Analysis. XPS was used to determine the coating surface chemical compositions at two photoelectron takeoff angles of 30° and 90°, corresponding to a probe depth of top 5 and 10 nm,[38,39] respectively. The high-resolution C_{1s} peak for the Q-2 coatings was curve fitted into five peaks (Figure 2b), according to the different carbon environments: C−C/C−H (~285 eV; its peak area was designated as A_1), C−O/C−N (~287 eV; A_2), C═O (~289 eV; A_3), CF_2 (~292 eV; A_4), and CF_3 (~294 eV; A_5). The F/C and N/C atomic ratios at the film surface can be calculated according to eqs 1 and 2, respectively.[40]

$$\frac{F}{C} = \frac{2A_4 + 3A_5}{\sum_{i=1}^{5} A_i} \quad (1)$$

DOI: 10.1021/acsami.5b04633
ACS Appl. Mater. Interfaces 2015, 7, 18467−18472

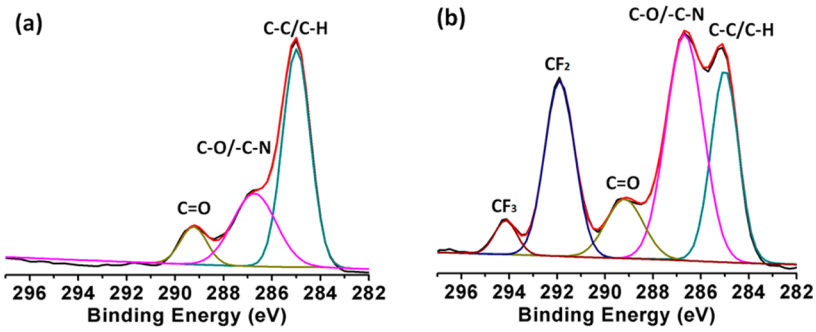

Figure 2. XPS C_{1s} signals for coatings at a takeoff angle of 30°: (a) Q-1 with about 0.96 mol % QAC-1, and (b) Q-2 with about 0.24 mol % QAC-2.

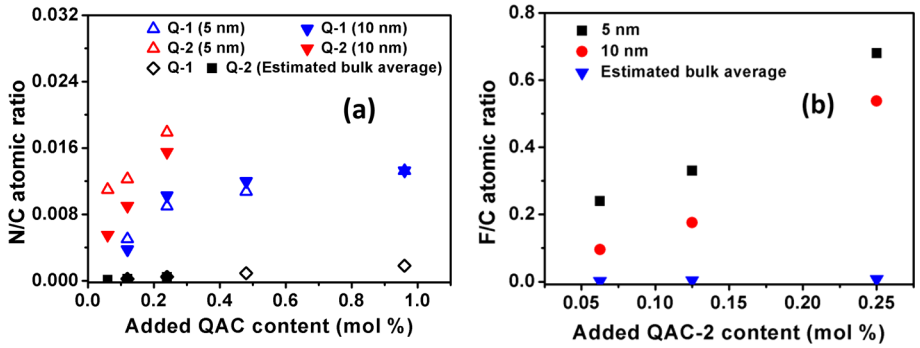

Figure 3. Surface atomic ratios: (a) N/C for both Q-1 and Q-2 coatings, and (b) F/C for Q-2 coatings in the top 5 and 10 nm of the coating as a function of the added QAC content (the estimated bulk average was added as the reference).

$$\frac{\mathrm{N}}{\mathrm{C}} = \frac{\frac{1}{4}(A_2 - A_3)}{\sum_{i=1}^{5} A_i} \tag{2}$$

Similarly, the C_{1s} peak for the Q-1 coatings can be curve fitted into three peaks (minus the two related to fluorocarbons, Figure 2a), and the N/C atomic ratio can be calculated below

$$\frac{\mathrm{N}}{\mathrm{C}} = \frac{\frac{1}{4}(A_2 - A_3)}{\sum_{i=1}^{3} A_i} \tag{3}$$

The surface chemical composition was compared with the calculated bulk ratio under the assumption of no QAC segregation. For the Q-1 coatings, the surface N/C ratio was greater than the estimated bulk average (Figure 3a), pointing to the surface segregation of QAC-1; for instance, the enrichment factor, namely, the ratio between the surface N/C ratio versus the estimated bulk average, was about 19 in the top 5 nm for the Q-1 coating with 0.24 mol % of QAC-1. However, the N/C ratios did not differ much with respect to the probing depth (5 vs 10 nm), implying that the QAC-1 surface enrichment was modest (compared to the Q-2 coatings). In contrast, the surface N/C ratio in the Q-2 series was significantly greater than the estimated bulk average (Figure 3a). Even at the low QAC-2 concentration of 0.24 mol %, the N/C ratio reached 0.018 in the top 5 nm (compared to the estimated bulk average ratio of 0.00046), representing an enrichment factor of about 39 and revealing much stronger surface enrichment of QAC-2 than QAC-1. In addition, there was an obvious difference for the N/C ratio at the 5 and 10 nm probing depths, further signifying the strong surface enrichment of QAC-2 at the coating surface.

The strong surface enrichment of QAC-2 in the Q-2 series was further confirmed by the F/C ratio at the coating surface (Figure 3b). A significant increase in the F/C ratio was observed in both the top 5 and the 10 nm of the coating, with a major difference between them, as the QAC-2 content increased in the coating. The surface enrichment factor on the basis of the F/C ratio for the coating with 0.24 mol % QAC-2 was estimated to be 85 and 68 in the top 5 and 10 nm, respectively. The enrichment factor from the surface F/C ratio was about twice as much as that from the surface N/C ratio at the same probe depth; this is logical considering that when a perfluoroalkyl QAC tail is enriched at the coating surface, the N atoms are more likely to be located underneath the more surface active fluorine atoms. The XPS analysis once again unequivocally confirmed that there was substantial segregation of the fluorinated QAC at the coating surface. The surface enrichment of QAC would in turn lead to strong antimicrobial property even at a very low overall QAC content, as will be demonstrated below. It should be pointed out that the increasing trend for the surface F/C ratio did not replicate that of the CA increase for hexadecane, since the CA of a liquid on the coating surface is more surface sensitive than the XPS technique.

Antimicrobial Activity. Antimicrobial activities of the coatings were evaluated by using the Gram-positive *S. epidermidis* and Gram-negative *E. coli* as the representative microorganisms, through the conventional test of bactericidal activity as described before,[35] in which the reduction of the number of viable bacterial cells (log scale) as colony-forming units (CFU) within 24 h incubation was recorded (Table 1). As the QAC-1 content increased in the Q-1 series, the coating became more potent in killing both Gram-positive and Gram-negative bacteria, eventually reaching 5-log reduction (total kill) at a QAC-1 concentration of 0.96 mol %.

Notably, all three Q-2 samples exhibited superior antimicrobial behavior against both *E. coli* and *S. epidermidis*, all with 5-

DOI: 10.1021/acsami.5b04633
ACS Appl. Mater. Interfaces 2015, 7, 18467−18472

log reductions for both bacteria. For the Q-2-A coating with only 0.06 mol % of QAC-2, its antimicrobial activity was as good as Q-1-D, a coating with as high as 0.96 mol % of QAC-1. This would not be surprising considering that the N/C atomic ratio in the top 5 nm was similar (~0.011) for the two coatings (Figure 3a). Therefore, it is not the overall QAC content in a coating but the surface QAC content that truly matters to render a coating highly antimicrobial; this is consistent with the previous finding that a higher cationic charge density at a surface usually led to more efficient antibacterial activity.[34] Use of a reactive perfluoroalkyl QAC has clearly demonstrated the advantage of our self-stratification strategy to significantly enrich the quaternary ammonium moiety at the coating surface, owing to the much lower surface energy of the perfluorinated tail, while the bulk property of the coating is expected to remain unchanged.

Zone of Inhibition Test. Release of antimicrobial agent from a coating may become an environmental hazard and trigger antibiotic resistance.[41] Therefore, nonleaching antimicrobial coatings with covalently bonded antimicrobial moieties are highly desired. To confirm that the introduced QAC moieties are not leached out from the Q-1 and Q-2 coatings, both coatings were subjected to a zone of inhibition test in the lawns of *E. coli* and *S. epidermidis*. As shown in Figure 4, no bacterial inhibition zone was observed around the

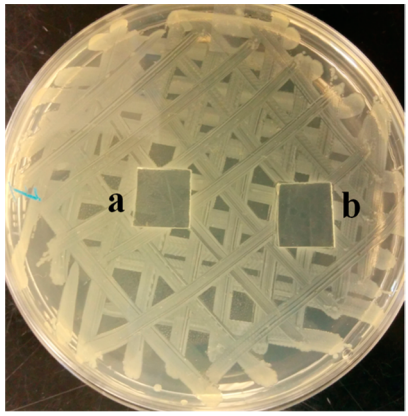

Figure 4. Picture of the zone of inhibition test result of samples (a) Q-1-D and (b) Q-2-C in *S. epidermidis* cultured lawn.

representative samples (Q-1-D and Q-2-C) against *S. epidermidis*, showing that no biocidal QAC species was leached out from the cross-linked coatings; otherwise, bacterial growth would be inhibited in a zone around the sample. The zone of inhibition test also revealed that the antimicrobial activity in our coatings was completely based on contact killing, not due to the release of any antimicrobial agent, which is again the consequence of covalently bonding the antimicrobial moieties to the cross-linked acrylic network.

CONCLUSIONS

By using a self-stratification strategy, we successfully developed excellent antimicrobial acrylic coatings via one-step UV curing of a mixture of acrylic monomers, including MMA, the cross-linker EGDMA, and a QAC-containing perfluoroalkyl monomer (QAC-2). The surface enrichment of the quaternary ammonium moiety was much more significant for the perfluorinated QAC than its hydrocarbon counterpart, QAC-1, owing to the low surface energy of the perfluoroalkyl tail. The QAC-2-containing Q-2 coatings demonstrated superior antimicrobial activity against both Gram-negative *E. coli* and Gram-positive *S. epidermidis* even at very low QAC-2 contents. The antimicrobial activity in our coatings was completely due to surface contact killing, and there was no leaching of free antimicrobial species. Due to the simplicity of our strategy and excellent antimicrobial activity at low QAC-2 contents, this type of coating may find wide applications in healthcare settings, food industry, biomedical industry, and other high-touch, high-risk environments.

AUTHOR INFORMATION

Corresponding Author

*E-mail: wming@georgiasouthern.edu.

Notes

The authors declare no competing financial interest.

ACKNOWLEDGMENTS

Financial support of this research at Georgia Southern University from USDA/NIFA (Award No. 2011-67022-30229) is gratefully acknowledged.

REFERENCES

(1) Guyomard, A.; Dé, E.; Jouenne, T.; Malandain, J.; Muller, G.; Glinel, K. Incorporation of a Hydrophobic Antibacterial Peptide into Amphiphilic Polyelectrolyte Multilayers: A Bioinspired Approach to Prepare Biocidal Thin Coatings. *Adv. Funct. Mater.* **2008**, *18*, 758−765.
(2) Waschinski, C.; Zimmermann, J.; Salz, U.; Hutzler, R.; Sadowski, G.; Tiller, J. Design of Contact-active Antimicrobial Acrylate-based Materials Using Biocidal Macromers. *Adv. Mater.* **2008**, *20*, 104−108.
(3) Schwartz, V.; Thetiot, F.; Ritz, S.; Putz, S.; Choritz, L.; Lappas, A.; Forch, R.; Landfester, K.; Jonas, U. Antibacterial Surface Coatings From Zinc Oxide Nanoparticles Embedded in Poly(*N*-isopropylacrylamide) Hydrogel Surface Layers. *Adv. Funct. Mater.* **2012**, *22*, 2376−2386.
(4) Asri, L.; Roest, C.; Chen, Y.; Ivashenko, O.; Rudolf, P.; Tiller, J.; Mei, H.; Loontjens, T.; Busscher, H. A Shape-adaptive, Antibacterial-coating of Immobilized Quaternary-ammonium Compounds Tethered on Hyperbranched Polyurea and Its Mechanism of Action. *Adv. Funct. Mater.* **2014**, *24*, 346−355.
(5) Zhao, J.; Song, L.; Shi, Q.; Luan, S.; Yin, J. Antibacterial and Hemocompatibility Switchable Polypropylene Nonwoven Fabric Membrane Surface. *ACS Appl. Mater. Interfaces* **2013**, *5*, 5260−5268.
(6) Lejars, M.; Margaillan, A.; Bressy, C. Fouling Release Coatings: A Nontoxic Alternative to Biocidal Antifouling Coatings. *Chem. Rev.* **2012**, *112*, 4347−4390.
(7) Li, Z.; Lee, D.; Sheng, X.; Cohen, R.; Rubner, M. Two-level Antibacterial Coating with both Release-killing and Contact-killing Capabilities. *Langmuir* **2006**, *22*, 9820−9823.
(8) Munoz-Bonilla, A.; Fernáandez-García, M. Polymeric Materials with Antimicrobial Activity. *Prog. Polym. Sci.* **2012**, *37*, 281−339.
(9) Aymonier, C.; Schlotterbeck, U.; Antonietti, L.; Zacharias, P.; Thomann, R.; Tiller, J.; Mecking, S. Hybrids of Silver Nanoparticles with Amphiphilic Hyperbranched Macromolecules Exhibiting Antimicrobial Properties. *Chem. Commun.* **2002**, 3018−3019.
(10) Sambhy, V.; MacBride, M.; Peterson, R.; Sen, A. Silver Bromide Nanoparticle/polymer Composites: Dual Action Tunable Antimicrobial Materials. *J. Am. Chem. Soc.* **2006**, *128*, 9798−9808.
(11) Kumar, A.; Vemula, P.; Ajayan, P.; John, G. Silver-nanoparticle-embedded Antimicrobial Paints Based on Vegetable Oil. *Nat. Mater.* **2008**, *7*, 236−241.
(12) Ho, C.; Tobis, J.; Sprich, C.; Thomann, R.; Tiller, J. Nanoseparated Polymeric Networks with Multiple Antimicrobial Properties. *Adv. Mater.* **2004**, *16*, 957−561.
(13) Rai, A.; Prabhune, A.; Perry, C. Antibiotic Mediated Synthesis of Gold Nanoparticles with Potent Antimicrobial Activity and Their

DOI: 10.1021/acsami.5b04633
ACS Appl. Mater. Interfaces 2015, 7, 18467−18472

Application in Antimicrobial Coatings. *J. Mater. Chem.* **2010**, *20*, 6789−6798.
(14) Vartiainen, J.; Tuominen, M.; Nattinen, K. Bio-hybrid Nanocomposite Coatings from Sonicated Chitosan and Nanoclay. *J. Appl. Polym. Sci.* **2010**, *116*, 3638−3647.
(15) Massi, L.; Guittard, F.; Levy, R.; Duccini, Y.; Geribaldi, S. Preparation and Antimicrobial Behaviour of Gemini Fluorosurfactants. *Eur. J. Med. Chem.* **2003**, *38*, 519−523.
(16) Harney, M.; Pant, R.; Fulmer, P.; Wynne, J. Surface Self-concentrating Amphiphilic Quaternary Ammonium Biocides as Coating Additives. *ACS Appl. Mater. Interfaces* **2009**, *1*, 39−41.
(17) Sun, Y.; Sun, G. Durable and Refreshable Polymeric *N*-halamine Biocides Containing 3-(4′-vinylbenzyl)-5,5-dimethylhydantoin. *J. Polym. Sci., Part A: Polym. Chem.* **2001**, *39*, 3348−3355.
(18) Eknoian, M.; Worley, S.; Bickert, J.; Williams, J. Novel Antimicrobial N-halamine Polymer Coatings Generated by Emulsion Polymerization. *Polymer* **1999**, *40*, 1367−1371.
(19) Sun, Y.; Sun, G. Novel Regenerable N-halamine Polymeric Biocides. I. Synthesis, Characterization, and Antibacterial Activity of Hydantoin-containing Polymers. *J. Appl. Polym. Sci.* **2001**, *80*, 2460−2467.
(20) Klibanov, A. Permanently Microbicidal Materials Coatings. *J. Mater. Chem.* **2007**, *17*, 2479−2482.
(21) Yagci, M.; Bolca, S.; Heuts, J.; Ming, W.; With, G. Antimicrobial Polyurethane Coatings Based on Ionic Liquid Quaternary Ammonium Compounds. *Prog. Org. Coat.* **2011**, *72*, 343−347.
(22) Kugel, A.; Stafslien, S.; Chisholm, B. Antimicrobial Coatings Produced by "Tethering" Biocides to the Coating Matrix: A Comprehensive Review. *Prog. Org. Coat.* **2011**, *72*, 222−252.
(23) Huang, J.; Murata, H.; Koepsel, R.; Russell, A.; Matyjaszewski, K. Immobilization of Amphiphilic Polycations by Catechol Functionality for Antimicrobial Coatings. *Biomacromolecules* **2007**, *8*, 1396−1399.
(24) Chen, C.; Beck-Tan, N.; Dhurjati, P.; van Dyk, T.; LaRossa, R.; Cooper, S. Quaternary Ammonium Functionalized Poly(propylene imine) Dendrimers as Effective Antimicrobials: Structure-activity Studies. *Biomacromolecules* **2000**, *1*, 473−480.
(25) Dizman, B.; Elasri, M.; Mathias, L. Synthesis and Characterization of Antibacterial and Temperature Responsive Methacrylamide Polymers. *Macromolecules* **2006**, *39*, 5738−5746.
(26) Kurt, P.; Wood, L.; Ohman, D.; Wynne, K. Highly Effective Contact Antimicrobial Surfaces via Polymer Surface Modifiers. *Langmuir* **2007**, *23*, 4719−4723.
(27) Yao, C.; Li, X.; Neoh, K.; Shi, Z.; Kang, E. Surface Modification and Antibacterial Activity of Electrospun Polyurethane Fibrous Membranes with Quaternary Ammonium Moieties. *J. Membr. Sci.* **2008**, *320*, 259−267.
(28) Thorsteinsson, T.; Masson, M.; Kristinsson, K.; Hjalmarsdottir, M.; Hilmarsson, H.; Loftsson, T. Soft Antimicrobial Agents: Synthesis and Activity of Labile Environmentally Friendly Long Chain Quaternary Ammonium Compounds. *J. Med. Chem.* **2003**, *46*, 4173−4181.
(29) Park, D.; Wang, J.; Klibanov, A. One-step, Painting-like Coating Procedures to Make Surfaces Highly and Permanently Bactericidal. *Biotechnol. Prog.* **2006**, *22*, 584−589.
(30) Ye, S.; Majumdar, P.; Chisholm, B.; Stafslien, S.; Chen, Z. Antifouling and Antimicrobial Mechanism of Tethered Quaternary Ammonium Salts in a Cross-linked Poly(dimethylsiloxane) Matrix Studied Using Sum Frequency Generation Vibrational Spectroscopy. *Langmuir* **2010**, *26*, 16455−16462.
(31) Kurt, P.; Wood, L.; Ohman, D.; Wynne, K. Highly Effective Contact Antimicrobial Surfaces via Polymer Surface Modifiers. *Langmuir* **2007**, *23*, 4719−4723.
(32) Tiller, J.; Liao, C.; Lewis, K.; Klibanov, A. Designing Surfaces that Kill Bacteria on Contact. *Proc. Natl. Acad. Sci. U. S. A.* **2001**, *98*, 5981−5985.
(33) Kenawy, E.; Worley, S.; Broughton, R. The Chemistry and Applications of Antimicrobial Polymers: A State-of-the-art Review. *Biomacromolecules* **2007**, *8*, 1359−1384.
(34) Murata, H.; Koepsel, R.; Matyjaszewski, K.; Russell, A. Permanent, Non-leaching Antibacterial Surfaces−2: How High Density Cationic Surfaces Kill Bacterial Cells. *Biomaterials* **2007**, *28*, 4870−4879.
(35) Yagci, M.; Bolca, S.; Heutsc, J.; Ming, W.; de With, G. Self-stratifying Antimicrobial Polyurethane Coatings. *Prog. Org. Coat.* **2011**, *72*, 305−314.
(36) van de Grampel, R.; Ming, W.; Gildenpfennig, A.; Laven, J.; Brongersma, H.; de With, G.; van der Linde, R. Quantification of Fluorine Density in the Outermost Atomic Layer. *Langmuir* **2004**, *20*, 145−149.
(37) van de Grampel, R.; Ming, W.; Gildenpfennig, A.; van Gennip, W.; Laven, J.; Niemantsverdriet, J.; Brongersma, H.; de With, G.; van der Linde, R. The Outermost Atomic Layer of Thin Films of Fluorinated Polymethacrylates. *Langmuir* **2004**, *20*, 6344−6351.
(38) Briggs, D. *Surface Analysis of Polymers by XPS and Static SIMS*; Cambridge University Press: Cambridge, 1998; Chapter 2.
(39) Kissa, E. *Fluorinated Surfactants: Synthesis, Properties, Applications*; Marcel Dekker: New York, 1993; p 386.
(40) Dikić, T.; Ming, W.; Thüne, P.; van Benthem, R.; de With, G. Well-defined Polycaprolactone Precursors for Low Surface-energy Polyurethane Films. *J. Polym. Sci., Part A: Polym. Chem.* **2008**, *46*, 218−227.
(41) Sun, X.; Zhang, L.; Cao, Z.; Deng, Y.; Liu, L.; Fong, H.; Sun, Y. Electrospun Composite Nanofiber Fabrics Containing Uniformly Dispersed Antimicrobial Agents as an Innovative type of Polymeric Materials with Superior Antimicrobial Efficacy. *ACS Appl. Mater. Interfaces* **2010**, *2*, 952−956.

DOI: 10.1021/acsami.5b04633
ACS Appl. Mater. Interfaces 2015, 7, 18467−18472